Pressure induced magnetic transition in siderite $FeCO_3$ studied by x-ray emission spectroscopy

2007 J. Phys.: Condens. Matter 19 386206

(http://iopscience.iop.org/0953-8984/19/38/386206)

IOP PUBLISHING JOURNAL OF PHYSICS: CONDENSED MATTER

J. Phys.: Condens. Matter **19** (2007) 386206 (8pp) doi:10.1088/0953-8984/19/38/386206

Pressure induced magnetic transition in siderite $FeCO_3$ studied by x-ray emission spectroscopy

A Mattila[1], T Pylkkänen[1,2], J-P Rueff[3,4], S Huotari[2], G Vankó[2,5], M Hanfland[2], M Lehtinen[6] and K Hämäläinen[1]

[1] Division of X-ray Physics, Department of Physical Sciences, University of Helsinki, POB 64, FI-00014, Finland
[2] European Synchrotron Radiation Facility, Boîte Postale 220, F-38043 Grenoble Cedex 9, France
[3] Laboratoire de Chimie Physique—Matière et Rayonnement, Université Pierre et Marie Curie—CNRS, 11 rue Pierre et Marie Curie, F-75005 Paris, France
[4] Synchrotron SOLEIL, L'Orme des Merisiers, BP-48 Saint-Aubin, F-91192 Gif-sur-Yvette, France
[5] KFKI Research Institute for Particle and Nuclear Physics, PO Box 49, H-1525 Budapest, Hungary
[6] Geological Museum, Finnish Museum of Natural History, University of Helsinki, POB 64, FI-00014, Finland

Received 5 June 2007, in final form 30 July 2007
Published 29 August 2007
Online at stacks.iop.org/JPhysCM/19/386206

Abstract

We have investigated the magnetic state of iron in siderite $FeCO_3$ under high pressure using Kβ x-ray emission spectroscopy. Pressure induced changes in the shape of the iron Kβ emission lines indicate that the iron ground state changes from a low pressure magnetic state to a high pressure non-magnetic state. This transition takes place roughly at 50 GPa. This conclusion is supported by charge transfer multiplet calculations of the iron Kβ emission line.

(Some figures in this article are in colour only in the electronic version)

1. Introduction

High pressure modifies several basic properties of materials such as crystalline and electronic structure, the dielectric, thermodynamical and transport properties. Transition metal ions with unfilled d shells are especially prone to electronic phase transitions at high pressures. The increase in the electronic density produced by the lattice compression changes the electron–electron interactions causing valence electron delocalization and magnetic transitions. In a localized picture of the transition metal ion's valence electrons, these magnetic transitions can be generally understood as transitions from a high spin (HS) to a low spin (LS) electronic state due to increased crystal field acting on the d electrons following the lattice compression.

Static high pressures can be generated using diamond anvil cells. The diamond anvil cell, however, places several restrictions on the spectroscopic tools available. Synchrotron radiation based x-ray techniques have been extensively used to study structural properties of matter under high pressure inside the diamond anvil cell and lately, spectroscopic tools have been applied to

investigate also dynamics and electronic structure. In electronic structure studies, the Kβ x-ray emission spectroscopy is now established as a local probe of the transition metal ion's magnetic state. As a hard x-ray method, the Kβ x-ray spectroscopy is also compatible with the diamond anvil cell techniques. Changes in the Kβ emission lineshape are related to the variation of the local spin magnetic moment and can be used to follow the evolution of the metal ion's magnetic state as a function of pressure.

Pressure induced magnetic transitions have been experimentally observed in various transition metal bearing compounds [1–8, 10–12] using high resolution x-ray emission spectroscopy (XES) besides optical and near-infrared absorption [14] and Mössbauer spectroscopy [9, 13]. Special interest has been bestowed on the properties of iron in various minerals [1, 3–5, 7–9, 14]. Especially the iron magnetic states in ferropericlase [5, 8, 9, 14] and silicate perovskites [7] have been extensively studied, since they directly influence the earth's lower mantle properties. The details of the magnetic transitions in these compounds are still very much under debate and further experimental data especially in relation to structural modifications at high pressures is needed. To shed more light on the details of the magnetic transitions in iron compounds, we have now extended these studies to siderite $FeCO_3$ mineral by following the evolution of the iron magnetic state under pressure using high resolution XES at the Kβ line.

The magnetic transitions have been approached theoretically very early on by using crystal field theory [15]. High pressure magnetism in transition metal oxides was later treated within the GGA method by considering the important d electrons as bandlike under pressure [16]. This approach, however, led in most cases to an overestimation of the transition pressure. Later work has treated the d electron correlation effects at high pressures using the LDA + U [17–19] and including the GGA approach [20–22]. Recently, also charge transfer multiplet calculations [23–25] have been applied to model XES spectra from transition metal oxides under high pressures [26] and been used to extract the relevant model parameters describing the electronic state of the metal ions. In this paper, we apply the charge transfer multiplet model to the analysis of the iron emission spectra from $FeCO_3$.

Siderite, $FeCO_3$, is a yellowish brown mineral commonly occurring in sedimentary iron ores. Siderite has a calcite structure, with the Fe^{2+} ions octahedrally coordinated by six oxygen atoms [27]. $FeCO_3$ is an antiferromagnet with a Néel temperature of $\simeq$38 K so that at room temperature the system is paramagnetic. The iron 2^+ ion is at the HS $S = 2$ state at ambient pressure [28] and we expect that by lattice compression the iron ion could be driven to a non-magnetic LS $S = 0$ state. Relatively few experiments probing the high pressure properties of $FeCO_3$ exist. The $FeCO_3$ calcite crystal structure has been found to be stable up to 50 GPa at room temperature [29], but no structural data on higher pressures has been published to our knowledge. In this paper we have extended this pressure range by measuring the Kβ emission from $FeCO_3$ sample from ambient pressure up to 88 GPa. We confirm that iron is at the HS state at ambient pressure and we find iron to undergo a magnetic transition to a high pressure non-magnetic LS state at around 50 GPa. This conclusion is supported by our computational modelling of the Kβ emission line.

2. Experimental details

We used a natural siderite mineral sample originating from the Ivigtut (Greenland) cryolite deposit. Selected samples were crushed in an agate mortar into a powder with an average particle size well below 5 μm. The structure and the elemental composition of the powdered sample was carefully checked using powder diffraction and x-ray fluorescence analysis. A small amount of impurities are usually present in natural siderite samples, often mostly in the

Table 1. Diamond anvil cell parameters for the different loadings. For all the loadings we used beveled diamonds with 300 μm culets with the flat diameter indicated in the table. The gasket material was rhenium in all cases.

Loading	Diamond culet flat (μm)	Gasket hole diameter (μm)	Pressure medium	Emission measured at pressures (GPa)
1	150	70	Argon	0.6, 30
2	150	70	None	40, 56, 71, 88
3	100	50	None	46

form of manganese, which substitutes iron in the crystal. The x-ray fluorescence analysis of the elemental composition confirmed the presence of a manganese impurity of about 4% of the iron concentration. This value is comparable to the number reported in the literature for the Ivigtut siderite deposit [27].

The Kβ x-ray emission experiments were carried out at the beamline ID16 of the European Synchrotron Radiation Facility. The incident radiation was monochromatized using a Si(111) double crystal monochromator and focused on the sample by a toroidal mirror into a spot size of 120 (horizontal) $\times$ 55 (vertical) μm^2. The excited x-ray emission from the sample inside the diamond anvil cell was analyzed in energy using a Rowland circle spectrometer with a vertical diffraction plane. A spherically bent Si(531) analyzer crystal with a 1 m bending radius was used. The vertical diffraction geometry allowed us to maintain the analyzer energy calibration and to accurately follow the position of the Kβ line since with the vertical scattering plane set-up the spectrometer energy calibration is not sensitive to small changes in the sample position along the incident x-ray beam.

Argon was used as a pressure medium in the first loading of the diamond anvil cell. For the second and third loading no pressure medium was used in order to maximize the fluorescence signal. It is possible that the lack of a pressure medium in the last two loadings led to some pressure gradient in the sample. For the first two loadings we used beveled diamond anvils with a 150 μm flat over a 300 μm culet. The third loading was done using beveled diamond anvils with a 100 μm flat over a 300 μm culet. We used Re gaskets pre-indented to approximately 20 μm with a roughly 70 μm hole for the first two loading and a 50 μm hole for the third loading. The diamond anvil cell parameters for the different loadings are summarized in table 1. Both the incident and emitted radiation passed through the diamond anvils and the Kβ emission was detected at a 30° scattering angle. The fluorescence was excited using incident radiation with a 12 keV energy to optimize the transmission of the incident radiation through the diamond and the resulting fluorescence count rate. The pressure was measured using the ruby fluorescence method before and after each x-ray emission measurement and was found to be stable within about 3 GPa. Emission spectra at 0.6 and 30 GPa were measured using the first loading, at 40, 56, 71 and 88 GPa using the second loading and at 46 GPa using the third loading.

3. Results and discussion

The evolution of the iron Kβ emission line as a function of pressure is shown in figure 1. The spectra are normalized to the integrated area. The Kβ emission ensues from a radiative decay of an iron 1s core hole to a 3p level. The Kβ emission spectrum is divided into a main line K$\beta_{1,3}$ and a satellite line Kβ' due to the exchange interaction between the 3p core hole and the unfilled 3d shell in the final state of the emission process. The K$\beta_{1,3}$ main line originates from the final states with the 3d shell net spin parallel to the open 3p^5 shell net spin

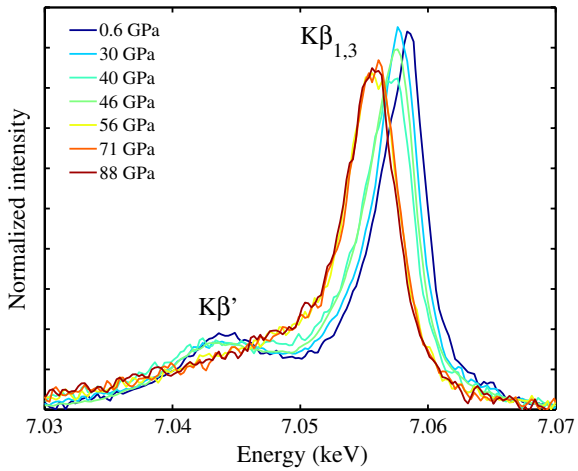

Figure 1. Evolution of the iron Kβ emission spectra from $FeCO_3$ as a function of pressure. The spectra have been normalized to the integrated intensity.

and the Kβ' satellite from the final states with the 3d shell net spin reverse to the $3p^5$ shell net spin [30, 31]. The energy separation between the satellite and the main line is proportional to the strength of the exchange interaction and the satellite intensity is proportional to the net spin of the 3d shell. Thus the intensity of the satellite is indicative of the spin magnetic moment, as established by numerous studies of 3d transition metal compounds. In figure 1 the emission lineshape shows a considerable change between 46 and 56 GPa with the intensity of the Kβ' satellite dropping and with the main emission line K$\beta_{1,3}$ position moving to lower emission energies. The observed collapse of the iron Kβ' satellite intensity in $FeCO_3$ above roughly 50 GPa pressure would, within the above qualitative picture of the emission process, indicate the loss of iron spin magnetic moment at high pressures.

Different approaches have been suggested to follow the extent of the spin transition using the Kβ emission spectra focusing on the variation of the satellite intensity [2], the full spectral shape [32], or the main peak position [7, 34]. These and other approaches have been critically reviewed in [33], and it was found that the integrated absolute value of the difference spectra (IAD) has the most merits for such analysis. Its crucial elements are (1) normalization to the spectral area, (2) shifting the spectra to the same center of mass [34], (3) subtracting a reference spectrum from all spectra, and integrating the absolute values of these difference spectra [32], and (4), converting the such determined IAD values to spin by projecting it on the spin scale spanned by reference spectra. In fortunate cases, the reference spectra are among the analyzed one, which is a typical case for pressure induced HS to LS transitions in Fe(II) compounds if high enough pressures are reached to make the transition complete. Application of such an inner references makes the analysis very reliable [35]; however, other reference compounds measured under similar conditions can also be used with success [12].

To compare the various methods used to follow the changes in the Kβ emission line, we report results obtained with three different analysis approaches: the above-described IAD, the K$\beta_{1,3}$ main line energy positions, and the satellite intensity. The latter is calculated on spectra aligned to the main peak position and normalized to the peak intensity, denoted as $I(K\beta')_{Pm}$ in [33], whose inaccuracy was found to be less than 10% [33]. Also, as discussed above, the vertical Rowland circle set-up allowed us to maintain the energy calibration of the spectrometer and to accurately extract the emission line energy positions.

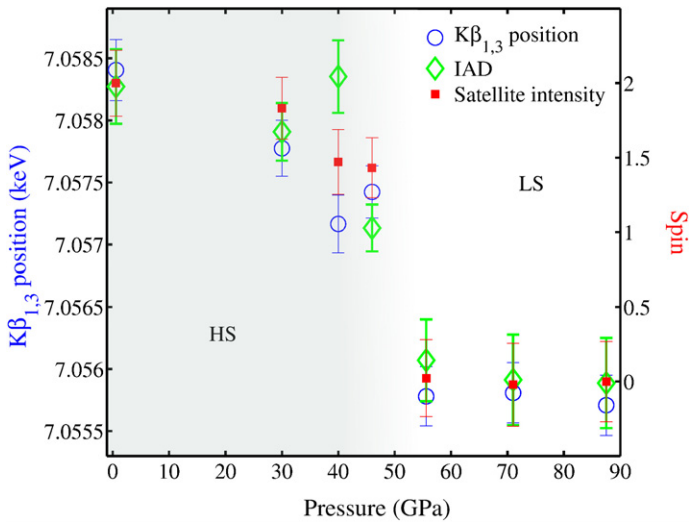

Figure 2. Position of the K$\beta_{1,3}$ peak (blue open circles), the integrated absolute difference values (green diamonds) of the Kβ emission line and the Kβ' satellite intensity as a function of pressure. The integrated absolute difference values and the satellite intensity values are scaled to the spin scale, given on the right vertical axis. The values divide into two branches, with the low pressure phase shaded.

Figure 2 shows the pressure induced variation of the spin determined from the Kβ emission spectra, together with the position of the K$\beta_{1,3}$ main peak. To calculate the IAD values, the average of three highest pressure spectra was used as a reference to further minimize statistical errors [35]. The lowest and highest pressure points of the satellite intensities are scaled to spin values 0 and 2, respectively, to relate the values to the spin scale. The error bars indicate the effects of limited statistics and the stability of the spectrometer energy calibration (stemming from beam or sample movements). The determined values from all approaches divide into two groups with an evident discontinuous change at around 50 GPa (the low pressure regime is shaded as a guide to the eye). The K$\beta_{1,3}$ position shifts about 1.5 eV to lower emission energy and the (average) spin value drops rapidly to 0 when crossing the ≈50 GPa boundary to the higher pressure side. The application of inner references for IAD is supported by the similarity of the 0.6 GPa spectrum to iron Fe^{2+} HS spectra and that of the 56–88 GPa spectra to a LS spectrum reported in the literature [1, 26, 33]. The transition is complete, as there is no further spectral evolution above 60 GPa with increasing pressure. These all indicate that at the ambient pressure the Fe^{2+} ions are indeed in the HS state with $S = 2$, and as the pressure is increased, a LS ground state configuration with $S = 0$ is reached. Also, the roughly 1.5 eV shift in the energy position of the K$\beta_{1,3}$ emission line towards lower energies when a non-magnetic state is reached is similar to what is observed in MnO with the loss of the manganese magnetic moment [10], and recalls the shift observed in the $(Fe, Mg)SiO_3$ perovskite with mixed Fe^{2+}/Fe^{3+} [7].

To further verify the nature of the magnetic transition and to elucidate the pressure induced changes in the electronic structure of iron, we used charge transfer multiplet calculations to model the evolution of the Kβ emission line [23–25]. In the charge transfer multiplet model, the effect of iron d electron hybridization with the octahedrally arranged nearest neighbor oxygens is considered using a configuration interaction scheme within the single impurity Anderson model [36]. For the iron 2^+ ion with a nominal valence of 6 d electrons we

Table 2. Parameters used in the calculations (in eV). The ground state configuration (HS/LS) is given in parenthesis after the pressure value. Charge transfer energy is given by Δ; V_{e_g} is the hybridization strength; $10Dq$ the crystal field splitting; U_{dc} the core hole Coulomb interaction; and W denotes the oxygen 2p bandwidth.

P (GPa)	Δ	V_{e_g}	$10Dq$	U_{dc}	W (O-2p)
0.6 (HS)	6.0	2.0	0.5	7.0	1.0
88 (LS)	7.0	3.2	1.2	7.0	7.0

considered a linear combination of $3d^6$ and $3d^7\underline{L}$ configurations for the ground state, with the $\underline{L}$ denoting a ligand hole. The calculations were made using O_h basis set at low and high pressures. In this basis set the iron 2^+ ion is either in the HS $^5T_2$ or in the LS $^1A_1$ ground state. The Slater integrals and spin–orbit parameters were calculated using the Hartree–Fock method [37], and the Slater integrals were further scaled down to 80% to account for the intra-atomic configuration interaction effects. Crystal field effects were considered using the approach developed by Butler [38] and charge transfer effects using the code by Thole and Ogasawara [24]. The Kβ emission spectra were calculated taking into account the term dependence of the final state lifetime broadening [39].

The model parameters were first set to reproduce the emission spectra at ambient (0.6 GPa) pressure. The parameters, charge transfer energy Δ (defined as the energy difference between the centers of gravities of $3d^6$ and $3d^7\underline{L}$ configurations), hybridization strength in the ground state V_{e_g}, the O-2p bandwidth W, and the crystal field splitting $10Dq$ are given in table 2. The parameter values are similar to those reported for FeO in [26], with the iron ground state in $FeCO_3$ being more ionic than in FeO. We used the same core hole Coulomb interaction U_{dc} for both $1\underline{s}$ and $3\underline{p}$ core hole states. The hybridization strength for the t_{2g} symmetry states $V_{t_{2g}}$ was set to half of the value for the e_g states V_{e_g} and for core hole states V_{e_g} was reduced by 0.4 eV from the ground state value. The term dependence of the final state lifetime broadening was approximated using a linear dependence ($-0.2 \times \omega$ full width at half-maximum) of the broadening on the fluorescence emission energy ω and finally the spectrum was convoluted with a 1.5 eV full width at half-maximum Gaussian to account for the instrumental broadening. To model the emission spectra at 88 GPa Δ, V_{e_g}, $10Dq$ and W were adjusted to fit the calculated spectra to the experiment, while freezing the core hole potentials, Slater integrals and lifetime broadening parameters to the ambient pressure values. The resulting parameters for the high pressure phase are also given in table 2.

The calculated spectra, shown together with the corresponding experimental emission spectra in figure 3, reproduce the pressure induced change in the emission line quite well. The calculation for the emission line at 88 GPa pressure reproduces the collapse of the emission line satellite and also roughly the shift in the main emission line position. The small underestimation of the satellite intensity at low emission energies at 88 GPa pressure is to some extent enhanced by the different positions of the experimental and calculated emission line maxima. The calculation confirms our earlier iron spin state assignments, below 50 GPa iron is in HS ground state and at higher pressures a transition to a LS ground state has taken place. Iron covalency effects in $FeCO_3$ at ambient pressure conditions have been found to be very small [40] and also at 0.6 GPa our calculations reveal the $3d^7\underline{L}$ configuration to have a relatively small weight of only 11% in the ground state. The large relative increase in the bandwidth W might be partly stemming from a possible underestimation of the bandwidth at low pressure. Otherwise, the lattice contraction is expected to increase the hybridization and crystal field splitting along with the bandwidth and the changes are within the lines observed in transition metal monoxides [26]. The charge transfer energy Δ, on the other hand, is relatively stable against the increasing

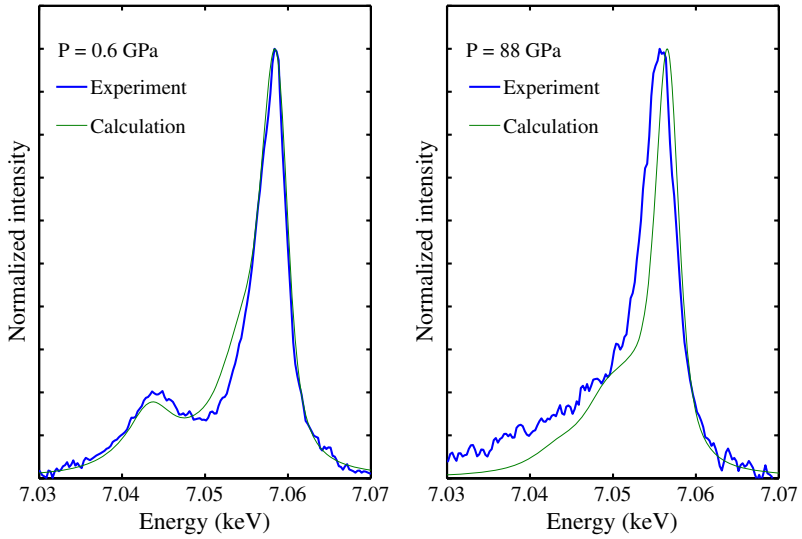

Figure 3. The experimental and calculated iron Kβ emission spectra from $FeCO_3$ at 0.6 GPa are shown in the left panel and at 88 GPa at the right panel. The spectra are normalized to maximum intensity in both panels to ease comparison.

pressure. A similar pressure dependence of Δ has been experimentally observed also in NiO [6].

4. Conclusions

We have measured the iron Kβ emission spectra from $FeCO_3$ as a function of pressure up to 88 GPa. At low pressures the iron 2^+ ion is in the HS ground state. Our analysis of the pressure induced changes in the emission lineshape using integrated absolute difference values, combined with charge transfer multiplet calculations, reveal that iron loses its magnetic moment and undergoes a transition into a non-magnetic LS phase at around 50 GPa. Our results demonstrate the versatility of the Kβ emission spectroscopy as a tool for studying the local magnetic properties of transition metal ions in different compounds and in various sample environments.

Acknowledgment

Financial support of the Academy of Finland (Contract No. 201291/205967/110571) is acknowledged.

References

[1] Rueff J-P, Kao C-C, Struzhkin V V, Badro J, Shu J, Hemley R J and Mao H-K 1999 *Phys. Rev. Lett.* **82** 3284
See also, Rueff J-P, Kao C-C, Struzhkin V V, Badro J, Shu J, Hemley R J and Mao H-K 1999 *Phys. Rev. Lett.* **83** 3343 (erratum)

[2] Rueff J-P, Krisch M, Cai Y Q, Kaprolat A, Hanfland M, Lorenzen M, Masciovecchio C, Verbeni R and Sette F 1999 *Phys. Rev.* B **60** 14510

[3] Badro J, Struzhkin V V, Shu J, Hemley R J, Mao H-K, Kao C-C, Rueff J-P and Shen G 1999 *Phys. Rev. Lett.* **83** 4101

[4] Badro J, Fiquet G, Struzhkin V V, Somayazulu M, Mao H-K, Shen G and Le Bihan T 2002 *Phys. Rev. Lett.* **89** 205504
[5] Badro J, Fiquet G, Guyot F, Rueff J-P, Struzhkin V V, Vankó G and Monaco G 2003 *Science* **300** 789
[6] Shukla A, Rueff J-P, Badro J, Vankó G, Mattila A, de Groot F M F and Sette F 2003 *Phys. Rev.* B **67** 081101(R)
[7] Badro J, Rueff J-P, Vankó G, Monaco G, Fiquet G and Guyot F 2004 *Science* **305** 383
[8] Lin J-F, Struzhkin V V, Jacobsen S D, Hu M Y, Chow P, Kung J, Liu H, Mao H-K and Hemley R J 2005 *Nature* **436** 377
[9] Speziale S, Milner A, Lee V E, Clark S M, Pasternak M P and Jeanloz R 2005 *Proc. Natl Acad. Sci. USA* **102** 17918
[10] Yoo C S, Maddox B, Klepeis J-H P, Iota V, Evans W, McMahan A, Hu M Y, Chow P, Somayazulu M, Häusermann D, Scalettar R T and Pickett W E 2005 *Phys. Rev. Lett.* **94** 115502
[11] Rueff J-P, Mattila A, Badro J, Vankó G and Shukla A 2005 *J. Phys.: Condens. Matter* **17** S717
[12] Vankó G, Rueff J-P, Mattila A, Németh Z and Shukla A 2006 *Phys. Rev.* B **73** 024424
[13] Kantor I Y, Dubrovinsky L S and McCammon C A 2006 *Phys. Rev.* B **73** 100101
[14] Goncharov A F, Struzhkin V V and Jacobsen S D 2006 *Science* **312** 1205
[15] Ohnishi S 1978 *Phys. Earth Planet. Inter.* **17** 130
[16] Cohen R E, Mazin I I and Isaak D G 1997 *Science* **275** 654
[17] Fang Z, Solovyev I V, Sawada H and Terakura K 1999 *Phys. Rev.* B **59** 762
[18] Gramsch S A, Cohen R E and Savrasov S Y 2003 *Am. Mineral.* **88** 257
[19] Tsuchiya T, Wentzovitch R M, da Silva C R S and de Gironcoli S 2006 *Phys. Rev. Lett.* **96** 198501
[20] Jiang X and Guo G Y 2004 *Phys. Rev.* B **69** 155108
[21] Cococcioni M, DalCorso A and de Gironcoli S 2003 *Phys. Rev.* B **67** 094106
[22] Rollmann G, Rohrbach A, Entel P and Hafner J 2004 *Phys. Rev.* B **69** 165107
[23] Kotani A and Shin S 2001 *Rev. Mod. Phys.* **73** 203
[24] de Groot F M F 2001 *Chem. Rev.* **101** 1779
[25] de Groot F M F 1994 *J. Electron Spectrosc. Relat. Phenom.* **670** 529
[26] Mattila A, Rueff J-P, Badro J, Vankó G and Shukla A 2007 *Phys. Rev. Lett.* **98** 196404
[27] Deers W A, Howie R A and Zussman J 1992 *An Introduction to the Rock-Forming Minerals* 2nd edn (England: Longman Scientific and Technical)
[28] Rueff J-P, Journel L, Petit P-E and Farges F 2004 *Phys. Rev.* B **69** 235107
[29] Santillán J and Williams Q 2004 *Phys. Earth Planet. Inter.* **143/144** 291
[30] Hämäläinen K, Kao C-C, Hastings J B, Siddons D P, Berman L E, Stojanoff V and Cramer S P 1992 *Phys. Rev.* B **46** 14274(R)
[31] Peng G, Wang X, Randall C R, Moore J A and Cramer S P 1994 *Appl. Phys. Lett.* **65** 2527
[32] Rueff J-P, Shukla A, Kaprolat A, Krisch M, Lorenzen M, Sette F and Verbeni R 2001 *Phys. Rev.* B **63** 132409
[33] Vanko G, Neisius T, Molnár G, Renz F, Kárpáti S, Shukla A and de Groot F M F 2006 *J. Phys. Chem.* B **110** 11647
[34] Glatzel P and Bergmann U 2005 *Coord. Chem. Rev.* **249** 65
[35] Vankó G and de Groot F M F 2007 *Phys. Rev.* B **75** 177101
[36] Anderson P W 1959 *Phys. Rev.* B **115** 2
[37] Cowan R D 1981 *The Theory of Atomic Structure and Spectra* (*Los Alamos Series in Basic and Applied Sciences*) (Berkeley, CA: University of California Press)
[38] Butler P 1981 *Point Group Symmetry Applications: Methods and Tables* (New York: Plenum)
[39] Taguchi M, Uozumi T and Kotani A 1997 *J. Phys. Soc. Japan* **66** 247
[40] Spiering H, Nagy D L and Zimmermann R 1976 *Chem. Phys.* **18** 243